Erzincan Üniversitesi
Fen Bilimleri Enstitüsü Dergisi
2025, 18(1), 248-263
ISSN: 1307-9085, e-ISSN: 2149-4584
Araştırma Makalesi

Erzincan University
Journal of Science and Technology
2025, 18(1), 248-263
DOI: 10.18185/erzifbed.1603785
Research Article

Frequency-Dependent Dielectric Characterization of $Bi_{1.75}Pb_{0.25}Sr_2Ca_2Cu_{3-x}Sn_xO_{10+\delta}$ Glass Ceramics System

Naki KAYA[1*], Haluk KORALAY[2]

[1]Kafkas University Kağızman Vocational School Department of Medical Service Optician Program Kars Turkey.
[2]Superconductivity and Thermal Analysis Laboratory (STAL), Department of Physics, Gazi University, 06531 Ankara, Turkey.

Received: 18/12/2024, **Revised:** 01/03/2025, **Accepted:** 05/03/2025, **Published:** 28/03/2025

Abstract

In this study, $Bi_{1.75}Pb_{0.25}Sr_2Ca_2Cu_{3-x}Sn_xO_{10+\delta}$ glass ceramic structure; (x = 0.0, 0.3, 0.5) depending on Cu_{3-x}-Sn_x displacement, frequency-dependent (100 Hz-2 MHz), capacitance-conductance measurements were taken at 75 K and 125 K temperature values. Dielectric constant reel part (ε'), imaginary dielectric constant (ε''), dielectric loss (tanδ) and ac electrical conductivity (σ_{ac}) frequency dependence were analyzed using the capacitance–voltage (*C–V*) and conductance-voltage (*G-V*) measurements. Sn doping had a negative capacitive effect and a decrease in capacitive effect was observed with the addition of Sn doping rate. The observed negative capacitance effect is believed to arise from the polarization effect generated by the Sn dopant. The negative dielectric constant and the virtual negative dielectric constant were calculated from the negative capacitance values. While the undoped sample exhibits a positive capacitance characteristic, the addition of Sn dopant to the samples results in the observation of a negative capacitance property. At the same time, it was found that the dielectric properties of the samples were dependent on frequency and temperature.

Keywords: Glass ceramic, negative capacitance, dielectric constant

$Bi_{1.75}Pb_{0.25}Sr_2Ca_2Cu_{3-x}Sn_xO_{10+\delta}$ Cam Seramik Sisteminin Frekans Bağımlı Dielektrik Karakterizasyonu

Öz

Bu çalışmada, $Bi_{1.75}Pb_{0.25}Sr_2Ca_2Cu_{3-x}Sn_xO_{10+\delta}$ cam seramik yapısı; (x=0.0, 0.3, 0.5) Cu_{3-x}-Sn_x yer değiştirmesine bağlı olarak, frekans bağımlı (100 Hz-2 MHz) kapasite ve iletkenlik ölçümleri 75 K ve 125 K sıcaklık değerlerinde alınmıştır. Dielektrik sabitin reel kısmı (ε'), sanal dielektrik sabit (ε''), dielektrik kayıp (tanδ) ve alternatif akım elektriksel iletkenlik (σ_{ac}) frekans bağımlılığı, kapasite-gerilim (*C-V*) ve iletkenlik-gerilim (*G-V*) ölçümleri kullanılarak analiz edilmiştir. Sn katkısı, negatif kapasite etkisi yaratmış ve Sn katkı oranının artışıyla kapasite etkisinde bir azalma gözlemlenmiştir. Gözlemlenen negatif kapasite etkisinin, Sn katkısı tarafından oluşturulan polarizasyon etkisinden kaynaklandığı düşünülmektedir. Negatif dielektrik sabiti ve sanal negatif dielektrik sabiti, negatif kapasite değerlerinden hesaplanmıştır. Katkılanmamış örnekler pozitif kapasite özelliği gösterirken, Sn eklenen örneklerde negatif kapasite özelliği gözlemlenmiştir. Aynı zamanda, örneklerin dielektrik özelliklerinin frekans ve sıcaklıkla bağımlı olduğu bulunmuştur.

Anahtar Kelimeler: Cam seramik, negative kapasitans, dielektrik sabit

*Corresponding Author: naki.kaya@kafkas.edu.tr
Naki KAYA, https://orcid.org/0000-0003-2287-676X
Haluk KORALAY, https://orcid.org/0000-0001-7893-344X

1. Introduction

Glasses and ceramics are classes of materials that have been the subject of research for a long time due to their unique mechanical and electrical properties, and they are important for many industrial, technological, and scientific applications. While glasses have an amorphous structure, ceramics have a crystalline structure. These two materials with different atomic arrangements have converged at a common point with glass-ceramic structures. Glass-ceramic materials will continue to attract attention for a long time due to their potential for application in various fields. Glass ceramics are commonly used in clinical applications [1], biomedical applications [2], and many other areas [3-6].

In glass-ceramic BSCCO systems, there are three different phases: $Bi_2Sr_2CuO_{6+y}$ (2201), $Bi_2Sr_2CaCu_2O_{8+y}$ (2212), and $Bi_2Sr_2Ca_2Cu_3O_{10+y}$ (2223) [7]. In the literature, it is possible to see that a wide range of different substances have been added during the production of BSCCO systems. Examples of these substances include Pb [8], Sb [9], Li [10], Nb [11], and Ga [12]. Although extensive research has been conducted on various physical properties of BSCCO glass ceramic systems, it is observed that the dielectric properties of these systems have not been sufficiently examined. Therefore, this study investigates the effect of Cu-Sn substitution on the dielectric properties of the BiSrCaCuO glass ceramic system.

In electrical circuits, capacitance is known as a property where charges are stored and electrical energy is accumulated. In addition to the conventional definition of capacitance, the existence of negative capacitance was mentioned in a study conducted in 1982 [13]. Subsequent research following the definition of negative capacitance revealed the presence of negative capacitance effects in various electronic systems [14-20]. Negative capacitance is highly important because it leads to a decrease in the charge on the electrodes as a result of the applied polarization voltage [21]. Negative capacitance is a complex physical phenomenon typically observed in ferroelectric materials. This phenomenon is based on a series of processes, such as energy level instabilities and the overcoming of energy barriers within the material. This property holds significant potential in low-power electronic devices, energy storage systems, and next-generation transistor technologies.

The concept of polarization is further divided into four fundamental groups: electronic (α_e), atomic or ionic (α_a), orientational or dipolar (α_o), and interfacial polarization (α_i). Each of these subgroups contributes to the overall polarization within the material's structure. Electronic polarization (α_e) involves the displacement of electrons within atomic or molecular orbits. α_a refers to the ability of atoms or ions within a material to shift from their equilibrium positions. α_o describes the alignment of permanent positive and negative charges in molecules separated by a distance, in response to an external electric field. α_i pertains to the appearance of polarization at interfaces between different phases of a material. Electronic polarization occurs at frequencies higher than 10^{15} Hz, atomic or ionic polarization is observed within the range of 10^{10}-10^{13} Hz, while dipolar or orientational polarization takes place in the intermediate range of 10^3-10^6 Hz. Interfacial polarization, on the other hand, occurs at frequencies lower than 10^3 Hz.

The electrical conduction mechanisms of electronic devices depend on various physical parameters. These parameters include temperature, frequency, surface charges, impurities, atomic defects, to name a few. The variation of these physical parameters can lead to the emergence of distinct dielectric properties in the studied sample. Therefore, when investigating frequency-dependent dielectric properties, it is advantageous to work across a wide frequency range. This approach allows for an examination over a broad spectrum of frequencies and can provide illuminating insights into the conduction and polarization mechanisms within the examined structure.

When reviewing the literature, it is evident that measurements of dielectric properties on BSCOO materials are quite limited. Therefore, the present study provides highly original data in this regard. These measurements and analyses offer a deeper understanding of the material's properties and contribute significantly to the existing body of knowledge in the field.

Due to its potential to revolutionize in technological advancements, the observation of negative capacitance effects in BSCCO systems is highly significant. To induce this effect, Cu-Sn substitution was carried out in the BiSrCaCuO system in this article. The analyses of the produced samples were conducted at two different temperature values, namely 75 K and 125 K, and within the frequency range of 100 Hz to 2 MHz.

2. Material and Methods

The samples in this study were produced using the melt-quencing method. Melt quenching is a widely utilized technique for the synthesis of amorphous materials, particularly glasses and certain polymers. This method is based on heating a substance to high temperatures until it reaches a molten state, followed by rapid cooling to solidify the material. The rapid cooling process (quenching) inhibits crystal formation, thereby facilitating the development of an amorphous structure. According to the desired composition of $Bi_{1.75}Pb_{0.25}Sr_2Ca_2Cu_{3-x}Sn_xO_{10+\delta}$, three different powder mixtures were obtained by substituting Cu with Sn (x: 0.0, 0.3, 0.5). The powders were then mixed and ground in an agate mortar for one hour to ensure homogeneity. The obtained mixtures were placed in an alumina crucible and heated in a furnace with a heating rate of 10 °C/min from room temperature to 1150 °C, where they were held for 90 minutes. After the heating process, the molten materials were poured between two pre-cooled copper plates. Rapid cooling resulted in the formation of black-colored glass with a thickness of approximately 0.6-0.8 mm. The obtained glasses were placed inside a tube furnace and sintered for 120 hours under oxygen flow at 830 °C. As a result of this process, three different samples with ceramic structure, depending on the Sn-Cu concentration, were obtained. The samples with doping ratios of 0.0, 0.3, and 0.5 were named $Sn_{0,0}$, $Sn_{0,3}$, and $Sn_{0,5}$, respectively. To obtain capacitance-conductance measurements, one surface of the fabricated samples was contacted to copper with silver paste. The other surface was masked and then contacted with copper wire and silver paste. Capacitance-conductance measurements were taken at temperatures of 75 K and 125 K over a frequency range of 100 Hz to 2 MHz. The measurements were performed using the Keithley 2400 SourceMeter and the Sourcetronic ST 2826 LCR Meter. The diode contact area was measured as 2 mm^2.

3. Result and Discussion

X-ray diffraction (XRD) analysis was conducted on the undoped sample to determine whether the obtained samples had an amorphous structure or not. XRD measurements were performed using a Rigaku Mini Flex 2 X-ray powder diffractometer with Cu-K_α radiation in the range of $10^0 \leq 2\theta \leq 70^0$. Figure 1 displays the XRD result obtained for the undoped sample.

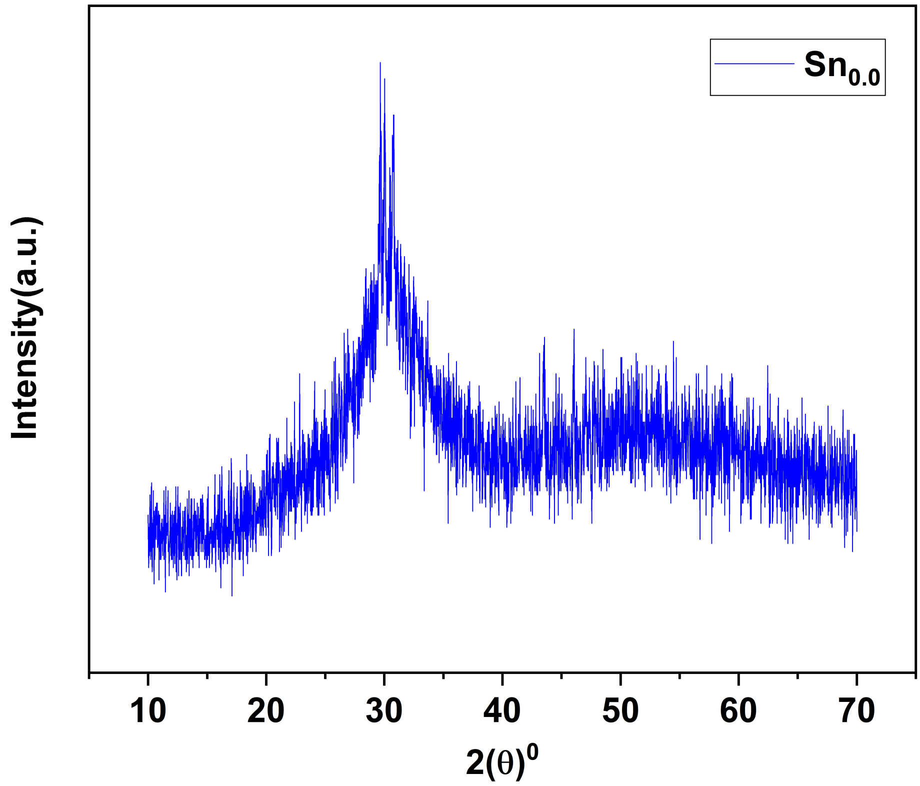

Fig. 1 XRD patterns of the undoped sample ($Sn_{0.0}$)

The atomic arrangement of glasses differs from the ordered atomic arrangement in crystalline structures, as they are randomly distributed. When the X-ray diffraction pattern is examined, a peak is observed at around 2θ=30°. As shown in Figure 1, a peak is indeed observed at 2θ=30°. This indicates the presence of a glassy structure.

The frequency dependence of ε', ε'', $tan\delta$, and σ_{ac} were evaluated based on the capacitance (C) and conductance (G) data obtained for the samples. Additionally, equations (1-4) were used in the calculations. ε' was calculated using equation 1.

$$C = \varepsilon' \varepsilon_0 \frac{A}{d} \tag{1}$$

where C is the capacitance of the sample (F), d is the thickness of the sample (m), ε_0 is the permittivity of free space ($\varepsilon_0 = 8.85 \times 10^{-12}$ F m^{-1}) and A is the area of the electrode (m^2). ε'' at various frequencies, was calculated using equation 2 based on the measured conductance values (G).

$$\varepsilon'' = \frac{d}{A\varepsilon_0} \frac{G}{2\pi f} \tag{2}$$

Here, G represents the conductance of the sample, ω (2πf) represents the angular frequency. $tan\delta$ was calculated using equation 3, while σ_{ac} was determined using equation 4.

$$\tan\delta = \frac{\varepsilon''}{\varepsilon'} \tag{3}$$

$$\sigma_{ac} = 2\pi f \varepsilon_0 \varepsilon' \tan\delta \tag{4}$$

Here, f represents the frequency of the applied alternating current field (in Hz).

Figure 2 depicts the variation of capacitance values with frequency for the prepared samples at 75 Kelvin, while Figure 3 illustrates the variation of capacitance values with frequency at 125 K.

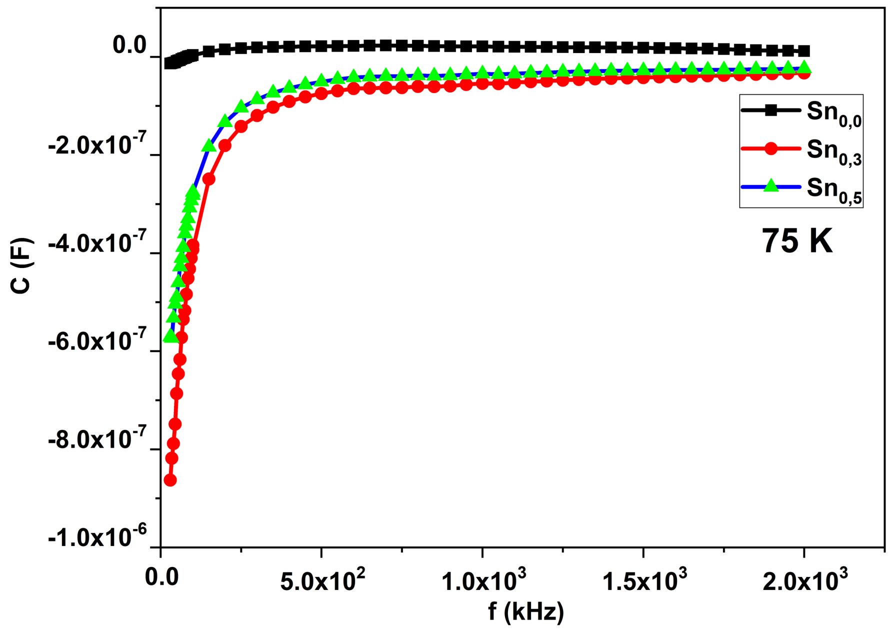

Fig. 2 The frequency dependency of the capacitance at 75 K

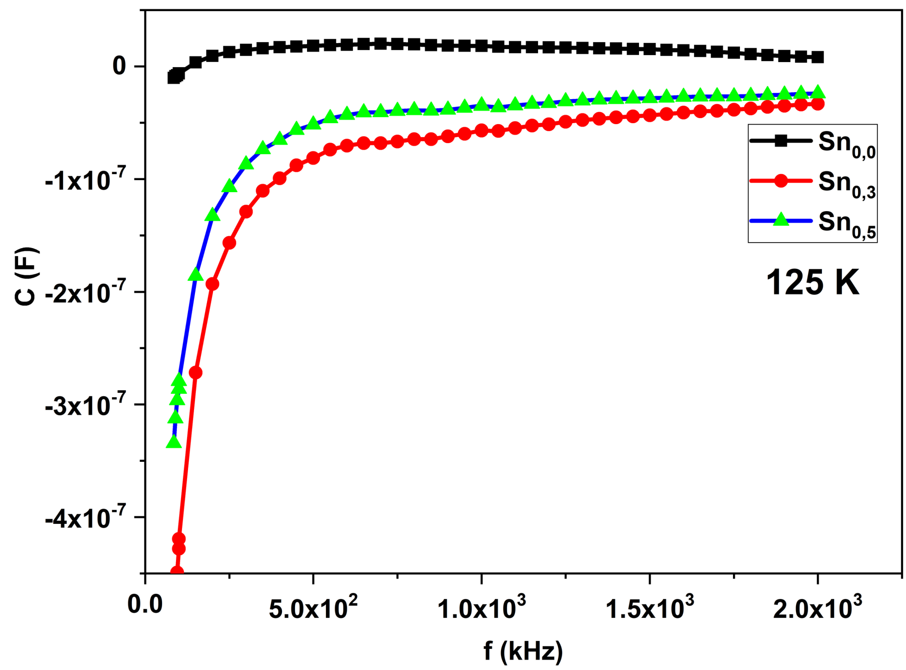

Fig. 3 The frequency dependency of the capacitance at 125 K

The capacitance values used in the obtained samples frequency-capacitance graphs are the data obtained from measurements. Upon examining Fig. 2 and Fig. 3, it is observed that the frequency-dependent capacitance variations change similarly at both temperatures. The obtained capacitance values are negative for all samples. This indicates the presence of a negative capacitance effect, which also plays a determining role in all other dielectric parameters. The frequency dependence of capacitance is more pronounced at low frequencies for all samples, and as the frequency increases, the frequency dependence of capacitance has decreased. The increase in the contribution ratio at both 75 K and 125 K leads to an increase in capacitive value, while no periodic correlation could be established for the undoped sample. In measurements taken at 125 K, the capacitance effect is observed to occur at higher frequencies compared to measurements taken at 75 K. This suggests that the measurement temperature plays a significant role in determining the capacitance value. The occurrence of negative capacitance values in Bi-based structures has been reported in previous studies [22]. In this context, it is observed that the measurement results are consistent with the literature. Figure 4 depicts the variation of conductance values with frequency for the prepared samples at 75 K, while Figure 5 illustrates the variation of conductance values with frequency at 125 K.

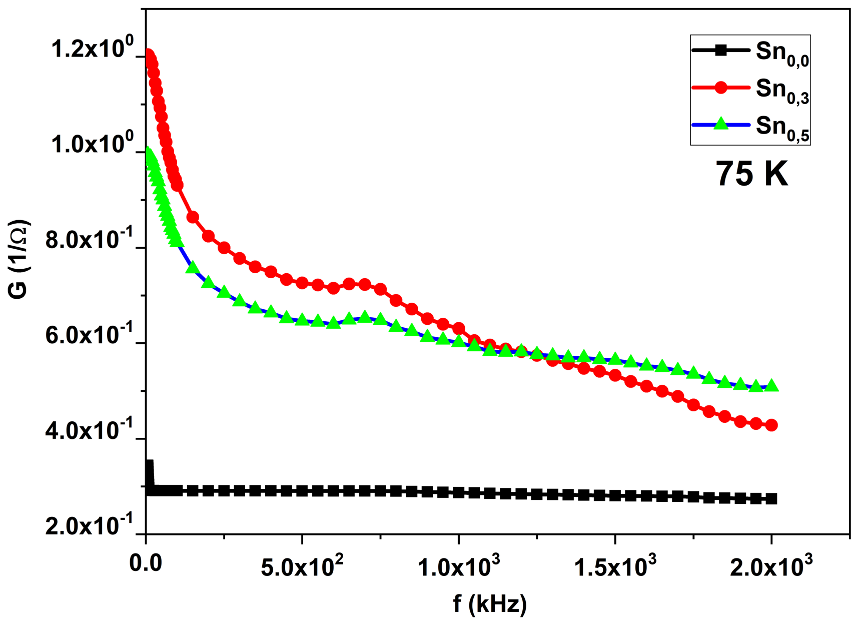

Fig. 4 The frequency dependency of the conductance at 75 K

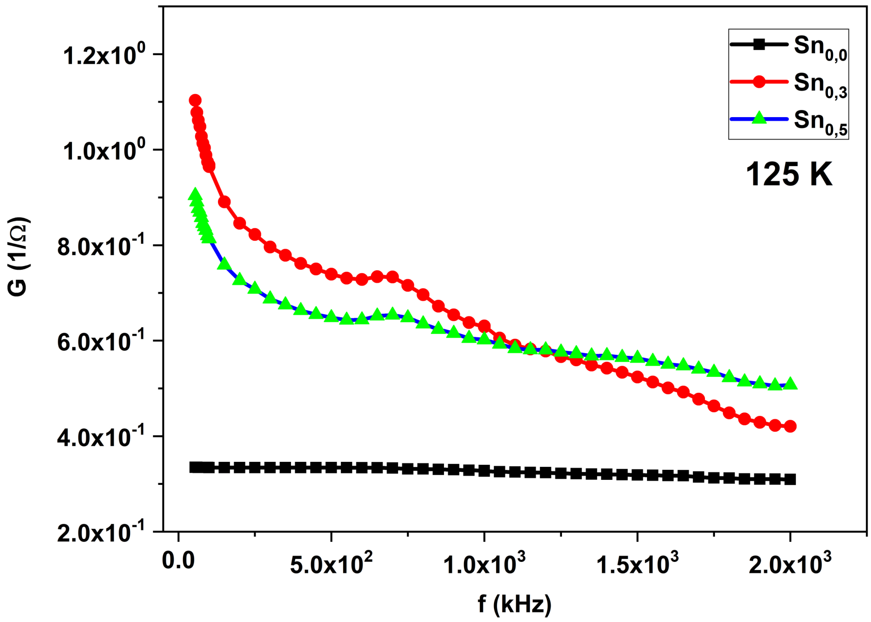

Fig. 5 The frequency dependency of the conductance at 125 K

When examining Figure 4 and Figure 5, it is observed that all samples exhibit similar behaviours. Physically, the increase in capacitance values would lead to a decrease in conductance. This observation is consistent with the literature [23]. Therefore, when Figures 2, 3, 4, and 5 are considered as a whole, consistent results are obtained that support each other. The increase in doping ratios across all samples has resulted in a decrease in conductance values. The frequency dependency of the ε' (75 K), ε' (125 K), ε'' (75 K), ε'' (125 K) and tan δ (75K), tan δ (125 K) of are shown in Figs. 6, 7, 8, 9, 10 and 11, respectively.

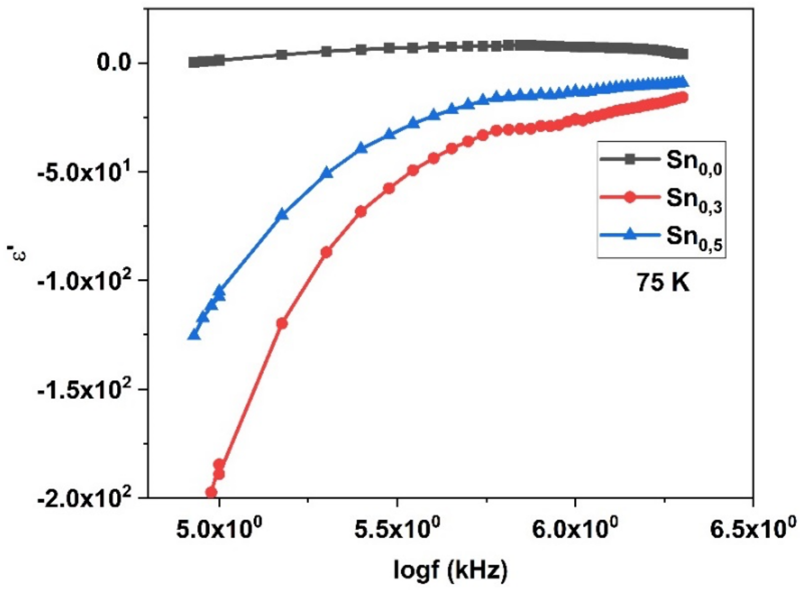

Fig. 6 The frequency dependency of the ε' at 75 K

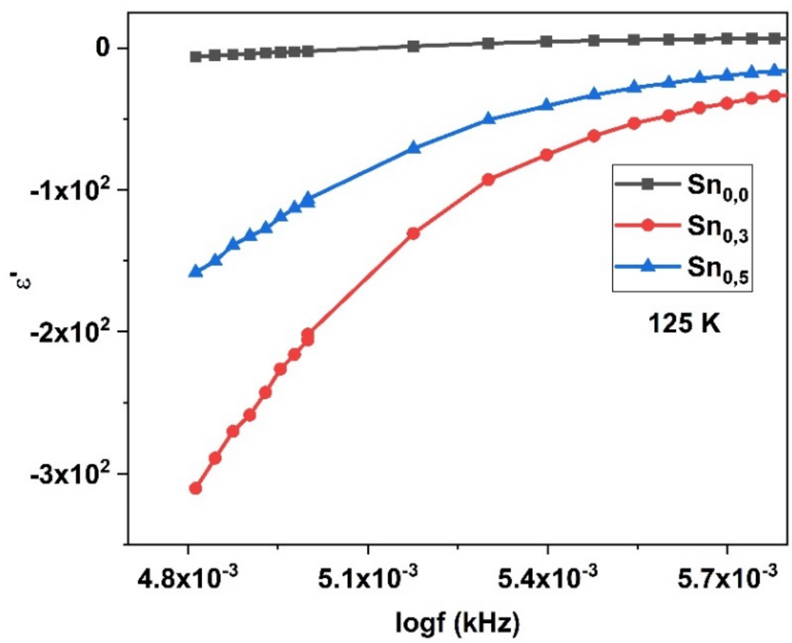

Fig. 7 The frequency dependency of the ε' at 125 K

Fig. 6 and Fig. 7 respectively illustrate the variation of the dielectric constant as a function of frequency at the temperature values of 75 K and 125 K. When these figures are examined, it can be observed that the change in dielectric constant shares a similar characteristic with the frequency-dependent capacitance change. The occurrence of negative values in the dielectric constant and the discovery of negative capacitance were predictable phenomena. The dielectric constant shows an increase with the increase in both temperatures, while no correlation has been established with the undoped sample. At 125 K, the samples have exhibited lower dielectric constant values compared to those at 75 K. In both temperature conditions, an increase in frequency for all doping ratios has led to an increase in the dielectric constant. At higher frequencies, a tendency of decrease in the dielectric constant values has been observed. The increase in capacitance and dielectric constant at high-frequency regions in the samples is attributed to the blocking of charge carriers at the electrodes [24]. When considering the increase in the value of dielectric constant, the total polarization effect should be taken into account.

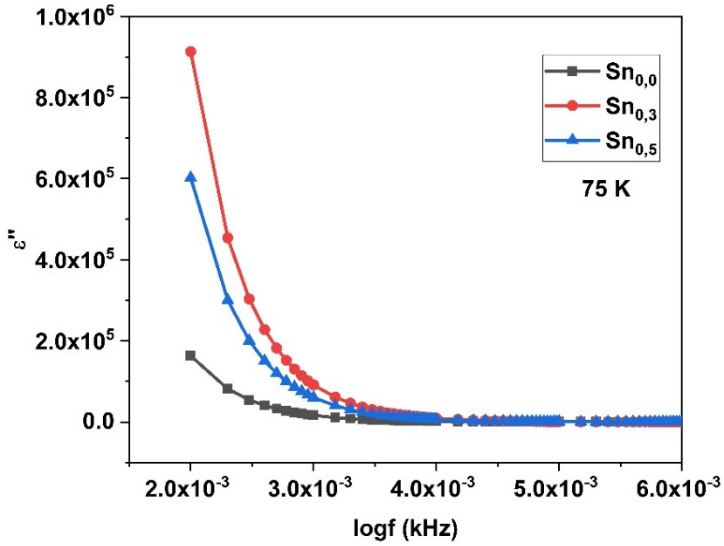

Fig. 8 The frequency dependency of the ε'' at 75 K

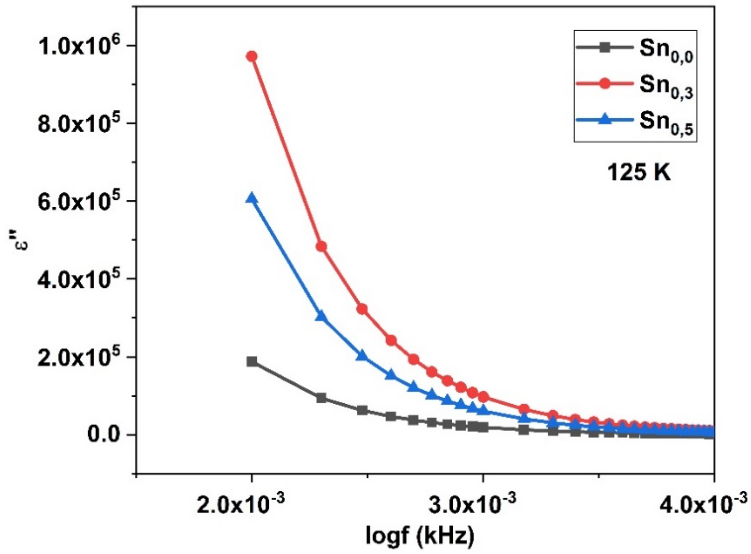

Fig. 9 The frequency dependency of the ε'' at 125 K

Upon examining Fig. 8 and Fig. 9, it can be observed that the variation of the ε'' value corresponds similarly to frequency changes both at 75 K and 125 K. The frequency-dependent change in ε'' value has followed a pattern similar to the frequency-dependent change in conductance. Likewise, while the ε' value tends to increase with increasing frequency, the ε'' value tends to decrease with increasing frequency. This is an expected behaviour. At low-frequency ranges, the increase in the contribution ratio at both temperatures has resulted in obtaining a lower ε'' value. As with other dielectric parameters, no correlation could be detected for the ε'' value in the case of the undoped sample. When a certain frequency value is exceeded, the ε'' values of all samples exhibit nearly identical changes. This situation is highly consistent with the literature [25-26].

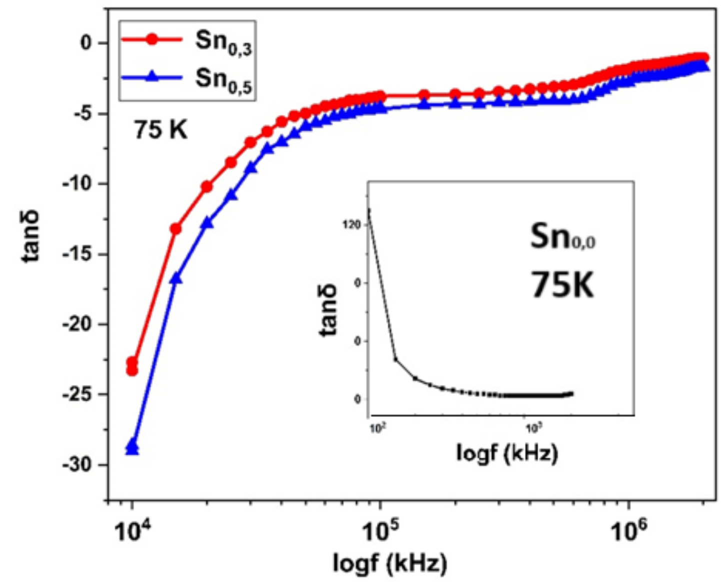

Fig. 10 The frequency dependency of the *tan δ* at 75 K

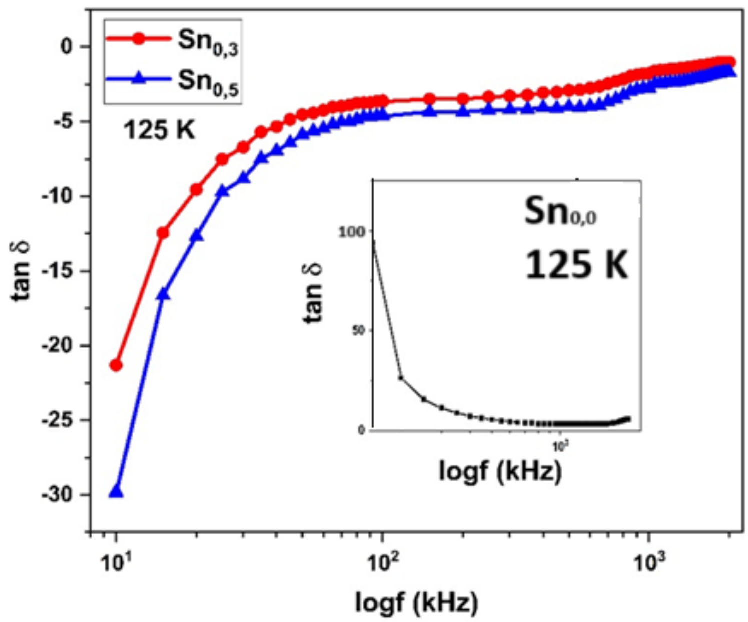

Fig. 11 The frequency dependency of the *tan δ* at 125 K

Dielectric loss is a measure of the energy dissipated per radian in the sample and is an important parameter for understanding the dielectric mechanism. When examining Fig. 10 and Fig. 11, it can be observed that dielectric loss is directly correlated with frequency. In the undoped sample, the dielectric loss value is in the positive range, whereas in the doped samples, this value is in the negative range. This observation is consistent with the other plotted graphs as well.

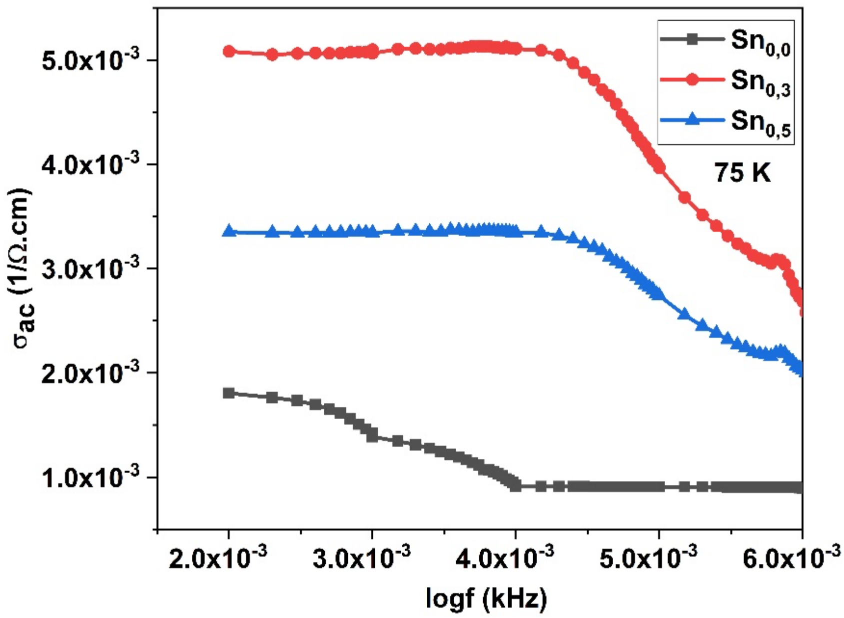

Fig. 12 The frequency dependency of the σ_{ac} at 75 K

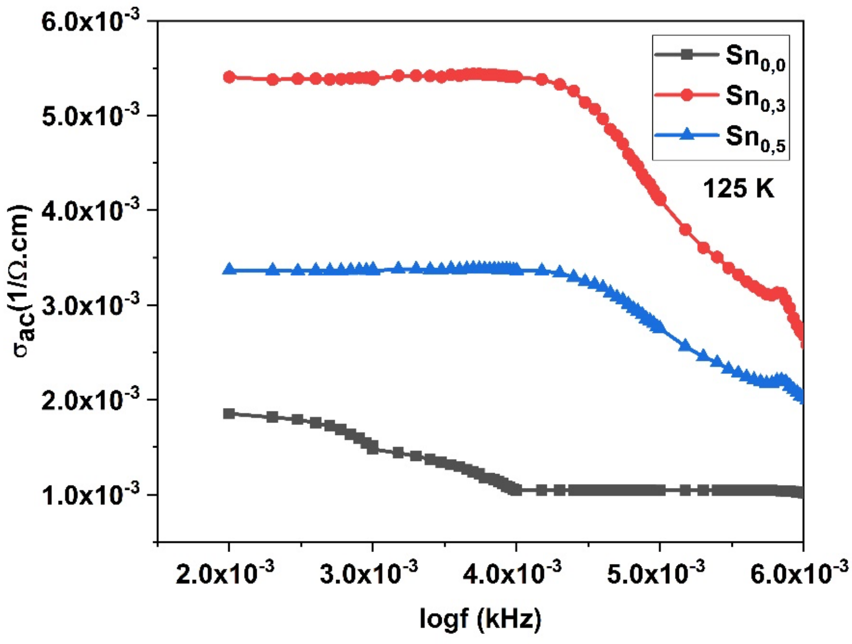

Fig. 13 The frequency dependency of the σ_{ac} at 125 K

When examining Figures 12 and Fig. 13, it can be observed that at high frequencies, the σ_{ac} values exhibit a trend towards linearity. This observation is consistent with the literature.

4. Conclusion

In this investigation, the glass ceramic structure of $Bi_{1.75}Pb_{0.25}Sr_2Ca_2Cu_{3-x}Sn_xO_{10+\delta}$ was studied, where (x=0.0, 0.3, 0.5) corresponding to different Cu_{3-x}-Sn_x displacements. Frequency-dependent measurements (ranging from 100 Hz to 2 MHz) of capacitance-conductivity were conducted at temperatures of 75 K and 125 K. The dependence of dielectric properties, including reel part of dielectric constant (ε'), imaginary part of dielectric constant (ε''), dielectric loss ($tan\delta$), and AC electrical conductivity (σ_{ac}), on frequency was analyzed using capacitance-voltage (C-V) and conductance-voltage (G-V) measurements, based on the Cu_{3-x}-Sn_x displacement.

In the obtained results, it was observed that the values of ε', ε'', $tan\delta$, and σ_{ac} are directly correlated with frequency and temperature. At all temperature and frequency values, the undoped sample exhibited a positive capacitance characteristic, whereas the doped samples displayed a negative capacitance feature. The frequency-dependent ε' parameter showed similar characteristics to the frequency-dependent capacitance value, while the frequency-dependent ε'' parameter exhibited similarities to the frequency-dependent conductance value. In this study, it is believed that the negative capacitance phenomenon observed in the samples is due to the hopping of carriers and dipolar polarization.

Ethics in Publishing

There are no ethical issues regarding the publication of this study.

Author Contributions

The authors did not declare any contrubution.

References

[1] Ritzberger, C., Apel, E., Höland, W., Peschke, A., Rheinberger, V. (2010). Properties and Clinical Application of Three Types of Dental Glass-Ceramics and Ceramics for CAD-CAM Technologies. Materials, 3(6), 3700–3713. doi:10.3390/ma3063700.

[2] Yokoi, T., Miyazaki, T., Kawashita, M., Ohtsuki, C. (2017). Bioactive Glass-Ceramics. Nanobioceramics For Healthcare Applications, 213-237. doi:10.1142/9781786341341_0008.

[3] Höland, W., Rheinberger, V., Apel, E., van't Hoen, C., Höland, M., Dommann, A., Graf-Hausner, U. (2006). Clinical applications of glass-ceramics in dentistry. Journal of Materials Science: Materials in Medicine, 17(11), 1037–1042. doi:10.1007/s10856-006-0441-y.

[4] Javed, H., Sabato, A., Dlouhy, I., Halasova, M., Bernardo, E., Salvo, M., Smeacetto, F. (2019). Shear Performance at Room and High Temperatures of Glass–Ceramic Sealants for Solid Oxide Electrolysis Cell Technology. Materials, 12(2), 298. doi:10.3390/ma12020298.

[5] Gallo, L. S., Villas Boas, M. O. C., Rodrigues, A. C. M., Melo, F. C. L., Zanotto, E. D. (2019). Transparent glass–ceramics for ballistic protection: materials and challenges. Journal of Materials Research and Technology. doi:10.1016/j.jmrt.2019.05.006.

[6] Singarapu, B., Galusek, D., Durán, A., Pascual, M. J. (2020). Glass-Ceramics Processed by Spark Plasma Sintering (SPS) for Optical Applications. Applied Sciences, 10(8), 2791. doi:10.3390/app10082791.

[7] Tarascon M. J., Le Page, Y., Crystal substructure and physical properties of the superconducting phase Bi4(Sr,Ca)6Cu4O16+x Phys. Rev. B, 37, 9382-9389 (1988). doi: 10.1103/PhysRevB.37.9382.

[8] Upadhyay, P. L., Rao, S. U. M., Nagpal, K. C., Sharma, R. G. (1992). Microstructures and the role of Pb in doped Bisrcacuo superconductor. Materials Research Bulletin, 27(1), 109–116. https://doi.org/10.1016/0025-5408(92)90048-5.

[9] Moon, B. M., Kordas, G., van Harlingen, D. J., Jeng, Y. L., Johnson, D. L., Sharpe, P. R., Goretta, K. (1991). Sinter-forge process for Pb,Sb-doped 110 K BiSrCaCuO superconducting phase. Materials Letters, 10(11-12), 481–484. https://doi.org/10.1016/0167-577X(91)90211-N.

[10] Schwartz, J., Wu, S. (1991). Effects of lithium doping on the formation and microstructure of bulk BiSrCaCuO. Physica C: Superconductivity, 190(1-2), 169–171. https://doi.org/10.1016/S0921-4534(05)80240-0.

[11] Li, Y., Yang, B., Liu, X., Li, Y. (1994). Effect of V, Nb, and Ta Doping on the 2223 Phase Formation and the Crystal Structure in the BiSrCaCuO System. Journal of Solid State Chemistry, 113(1), 176–181. doi: 10.1006/jssc.1994.1357.

[12] Gridin, V. V., Ummat, P. K., Datars, W. R. (1992). Paraconductivity of Ga-doped BiPbSrCaCuO. Journal of Physics: Condensed Matter, 4(3), 823–828. doi: 10.1088/0953-8984/4/3/021.

[13] Sandoval, F., Lopez, C., Munoz, E. (1982). Forward-bias impedance of $GaAs_{1-x}P_x$ LED's. Solid-State Electronics, 25, 355-357. doi: 10.1016/0038-1101(82)90119-8.

[14] Wu, X., Yang, E. S., Evans, H. L. (1990). Negative capacitance at metal-semiconductor interfaces. Journal of Applied Physics, 68(6), 2845–2848. doi:10.1063/1.346442.

[15] Champness, C. H., Clark, W. R. (1990). Anomalous inductive effect in selenium Schottky diodes. Applied Physics Letters, 56(12), 1104–1106. doi:10.1063/1.102581.

[16] Wang, C. C., Liu, G. Z., He, M., Lu, H. B. (2008). Low-frequency negative capacitance in $La_{0.8}Sr_{0.2}MnO_3$/Nb-doped $SrTiO_3$ heterojunction. Applied Physics Letters, 92(5), 052905. doi:10.1063/1.2840195.

[17] Perera, A. G. U., Shen, W. Z., Ershov, M., Liu, H. C., Buchanan, M., Schaff, W. J. (1999). Negative capacitance of GaAs homojunction far-infrared detectors. Applied Physics Letters, 74(21), 3167–3169. doi:10.1063/1.124169.

[18] Feng, L. F., Li, D., Zhu, C. Y., Wang, C. D., Cong, H. X., Xie, X. S., Lu, C. Z. (2007). Simultaneous sudden changes of electrical behavior at the threshold in laser diodes. Journal of Applied Physics, 102(6), 063102. doi:10.1063/1.2779278.

[19] Zhu, C. Y., Feng, L. F., Wang, C. D., Cong, H. X., Zhang, G. Y., Yang, Z. J., Chen, Z. Z. (2009). Negative capacitance in light-emitting devices. Solid-State Electronics, 53(3), 324–328. doi:10.1016/j.sse.2009.01.002.

[20] Zaidi, S. H., & Jonscher, A. K. (1987). Spectroscopy of delayed electronic transitions in GaAs Schottky diodes. Semiconductor Science and Technology, 2(9), 587–596. doi:10.1088/0268-1242/2/9/005.

[21] Ehrenfreund, E., Lungenschmied, C., Dennler, G., Neugebauer, H., & Sariciftci, N. S. (2007). Negative capacitance in organic semiconductor devices: Bipolar injection and charge recombination mechanism. Applied Physics Letters, 91(1), 012112. doi:10.1063/1.2752024.

[22] Ş. Çavdar, H. Koralay, Ş. Altındal. Effect of Vanadium Substitution on the Dielectric Properties of Glass Ceramic Bi-2212 Superconductor. J Low Temp Phys (2011) 164:102–114 DOI 10.1007/s10909-011-0361-1.

[23] Padma, R., Lakshmi, B. P., Reddy, V. R. (2013). Capacitance–frequency (C–f) and conductance–frequency (G–f) characteristics of Ir/n-InGaN Schottky diode as a function of temperature. Superlattices and Microstructures, 60, 358–369. doi:10.1016/j.spmi.2013.05.014.

[24] Çavdar, Ş., Koralay, H., Tuğluoğlu, N., Günen, A. (2005). Frequency-dependent dielectric characteristics of Tl–Ba–Ca–Cu–O bulk superconductor. Superconductor Science and Technology, 18(9), 1204–1209. doi:10.1088/0953-2048/18/9/010.

[25] Lal, B., Bamzai, K. K., Kotru, P. N., & Wanklyn, B. M. (2004). Microhardness, fracture mechanism and dielectric behaviour of flux-grown $GdFeO_3$ single crystals. Materials Chemistry and Physics, 85(2-3), 353–365. doi:10.1016/j.matchemphys.2004.01.

[26] Reddy A V R, Mohan R G, Ravinder P and Boyanov B S (1999). High-frequency dielectric behaviour of polycrystalline zinc substituted cobalt ferrites. Journal of Materials Science, 34, 3169–3176.